Chapter 5

Chiral Perturbation Theory and the δ-regime

As it was mentioned in Chapter 2, the low energy level of QCD cannot be treated with perturbation theory, but one can use lattice simulations. The most successful analytic approach to this regime is *Chiral Perturbation Theory*, which is an effective field theory. The Lagrangian of the effective theory is built by introducing a field in the coset space of the symmetry breaking group and by adding all the terms that are consistent with the symmetries of the underlying theory (QCD). This leads us to a consideration of the chiral symmetry of the QCD Lagrangian.

5.1 QCD chiral symmetry

Since we are interested in low energy, we will work with the flavors whose masses satisfy $m_f \ll \Lambda_{\text{QCD}} \approx 300$ MeV. Therefore we only take into account the u and d quarks, with masses in the following range [1]

$$\begin{aligned} m_u &= 1.9 \text{ - } 2.65 \text{ MeV}, \\ m_d &= 4.5 \text{ - } 5.15 \text{ MeV}. \end{aligned} \tag{5.1}$$

Then, in Minkowski space-time, the QCD Lagrangian is given by

$$\begin{aligned} \mathcal{L} &= \sum_{f=u,d} (\overline{q}_f i\gamma^\mu D_\mu q_f - m_f \overline{q}_f q_f) - \frac{1}{4}\text{tr}\left[G_{\mu\nu}G^{\mu\nu}\right], \\ D_\mu &= (\partial_\mu + igA_\mu), \;\; G_{\mu\nu} = \partial_\mu A_\nu - \partial_\nu A_\mu + ig[A_\mu, A_\nu], \end{aligned} \tag{5.2}$$

where q_f and $\overline{q}_f$ are independent Grassmann fields associated with the flavor f with mass m_f and where the gauge field is $A_\mu(x) = \sum_{a=1}^{8} A_\mu^a(x) T_a$, where A_μ^a are in general complex numbers and T_a are the basis elements of the traceless Hermitian 3×3 matrices (generators of SU(3)). This implies that the gauge field is a matrix as well. The Lagrangian is constructed in the same way as we did in Section 2.3, so it is invariant under SU(3) gauge transformations. We are interested in analyzing the chiral symmetry, therefore we apply the chiral projection operators

$$P_R = \frac{1}{2}(\mathbb{I} + \gamma_5), \;\; P_L = \frac{1}{2}(\mathbb{I} - \gamma_5) \tag{5.3}$$

to the quark fields in order to obtain the right-handed and left-handed fields

$$q_{R_f} = P_R q_f, \;\; q_{L_f} = P_L q_f, \;\; \overline{q}_{R_f} = \overline{q}_f P_L, \;\; \overline{q}_{L_f} = \overline{q}_f P_R. \tag{5.4}$$

By using $\{\gamma_5, \gamma^\mu\} = 0$, $\gamma_5^2 = \mathbb{I}$, $\gamma_5^\dagger = \gamma_5$ and the definition of the chiral operators one can show the following properties

$$P_{L,R} = P_{L,R}^\dagger, \;\; P_{L,R}^2 = P_{L,R}, \;\; P_R P_L = P_L P_R = 0, \;\; P_{R,L}\gamma^\mu = \gamma^\mu P_{L,R}. \tag{5.5}$$

Then

$$\begin{aligned} q_f &= q_{R_f} + q_{L_f}, \\ \overline{q}_f &= \overline{q}_{R_f} + \overline{q}_{L_f}. \end{aligned} \tag{5.6}$$

With eqs. (5.5) and eqs. (5.6) the QCD Lagrangian takes the form

$$\mathcal{L} = \sum_{f=u,d} \left[\overline{q}_{L_f} i\gamma^\mu D_\mu q_{L_f} + \overline{q}_{R_f} i\gamma^\mu D_\mu q_{R_f} - m_f(\overline{q}_{R_f} q_{L_f} + \overline{q}_{L_f} q_{R_f}) \right] - \frac{1}{4}\mathrm{tr}\left[G_{\mu\nu}G^{\mu\nu}\right]. \tag{5.7}$$

Now, we use global chiral transformations defined by

$$q_{R,L_f} \to q'_{R,L_f} = e^{i\alpha\gamma_5} q_{R,L_f}, \;\; \overline{q}_{R,L_f} \to \overline{q}'_{R,L_f} = \overline{q}_{R,L_f} e^{i\alpha\gamma_5}, \;\; \alpha \in \mathbb{R}. \tag{5.8}$$

The mass term is not invariant under these transformations, so for the moment we will set $m = 0$. On the other hand, since $\{\gamma^\mu, \gamma_5\} = 0$ it follows that $\gamma^\mu e^{i\alpha\gamma_5} = e^{-i\alpha\gamma_5}\gamma^\mu$. As a result the Lagrangian transforms as

$$\begin{aligned} \mathcal{L} &= \sum_{f=u,d} \left(\overline{q}_{L_f} i\gamma^\mu D_\mu q_{L_f} + \overline{q}_{R_f} i\gamma^\mu D_\mu q_{R_f} \right) - \frac{1}{4}\mathrm{tr}\left[G_{\mu\nu}G^{\mu\nu}\right] \\ &= \sum_{f=u,d} \left(\overline{q}'_{L_f} i\gamma^\mu D_\mu q'_{L_f} + \overline{q}'_{R_f} i\gamma^\mu D_\mu q'_{R_f} \right) - \frac{1}{4}\mathrm{tr}\left[G_{\mu\nu}G^{\mu\nu}\right]. \end{aligned}$$

Hence, $\mathcal{L}$ is invariant under the transformations of eq. (5.8) only when $m = 0$, for that reason this is called the chiral limit.

If we express the quark fields as vectors

$$q_{R,L} = \begin{pmatrix} q_{R,L_u} \\ q_{R,L_d} \end{pmatrix}, \;\; \overline{q}_{R,L} = \left(\overline{q}_{R,L_u}, \overline{q}_{R,L_d} \right), \;\; q = \begin{pmatrix} q_u \\ q_d \end{pmatrix}, \;\; \overline{q} = \left(\overline{q}_u, \overline{q}_d \right), \tag{5.9}$$

we can rewrite the Lagrangian as

$$\mathcal{L} = \overline{q}_L i\gamma^\mu D_\mu q_L + \overline{q}_R D_\mu q_R - \frac{1}{4}\mathrm{tr}\left[G_{\mu\nu}G^{\mu\nu}\right] \tag{5.10}$$

and apply separate global U(2) transformations

$$\begin{aligned} q_R \to q'_R = R\, q_R, \quad \overline{q}_R \to \overline{q}'_R = \overline{q}_R R^\dagger, \quad R \in \mathrm{U}(2)_R, \\ q_L \to q'_L = L\, q_L, \quad \overline{q}_L \to \overline{q}'_L = \overline{q}_L L^\dagger, \quad L \in \mathrm{U}(2)_L. \end{aligned} \tag{5.11}$$

Under these transformations, $\mathcal{L}$ is once again invariant. The corresponding symmetry group is $\mathrm{U}(2)_L \otimes \mathrm{U}(2)_R$. An element of U(2) can be decomposed into an element of SU(2) multiplied by a phase factor, thus

$$\mathrm{U}(2)_L \otimes \mathrm{U}(2)_R = \mathrm{SU}(2)_L \otimes \mathrm{SU}(2)_R \otimes \mathrm{U}(1)_B \otimes \mathrm{U}(1)_A, \tag{5.12}$$

where $\mathrm{U}(1)_A$ is the axial symmetry, which is broken explicitly under quantization (axial anomaly). $\mathrm{U}(1)_B$ is associated with the baryon number conservation, while $\mathrm{SU}(2)_L \otimes$

$\mathrm{SU}(2)_R$ is the chiral symmetry group. The latter breaks spontaneously to SU(2). We analyze this through the chiral condensate

$$\langle 0|\,\overline{q}q\,|0\rangle = \langle 0|\,\overline{q}_R q_L + \overline{q}_L q_R\,|0\rangle\,. \tag{5.13}$$

Under the transformations in eq. (5.11) the chiral condensate transforms as

$$\langle 0|\,\overline{q}'q'\,|0\rangle = \langle 0|\,\overline{q}_R R^\dagger L q_L + \overline{q}_L L^\dagger R q_R\,|0\rangle\,, \tag{5.14}$$

where we see that only if $R = L$, $\langle 0|\,\overline{q}q\,|0\rangle$ remains invariant. Hence, we have the following spontaneous breaking pattern

$$\mathrm{SU}(2)_L \otimes \mathrm{SU}(2)_R \to \mathrm{SU}(2)_{L=R}. \tag{5.15}$$

The order parameter of this broken symmetry is $\langle 0|\,\overline{q}q\,|0\rangle$, so when it is different from zero the chiral symmetry is indeed spontaneously broken. Because of the Goldstone theorem, this broken symmetry corresponds to

$$\dim(\mathrm{SU}(2)_L \otimes \mathrm{SU}(2)_R) - \dim(\mathrm{SU}(2)) = 3 + 3 - 3 = 3 \tag{5.16}$$

massless Nambu-Goldstone Bosons (NGB). If now we take into account the masses m_u and m_d, the symmetry is explicitly broken and the NGBs turn into light massive quasi NGBs, which can be identified with the pion triplet π^+, π^-, π^0. See refs. [2, 3, 4] for further details.

5.2 Effective Lagrangian

In order to build the effective Lagrangian $\mathcal{L}_{\text{eff}}$, one introduces a field $U(x)$ in the coset space of the symmetry breaking group, *i.e.*

$$U(x) \in (\mathrm{SU}(2)_L \otimes \mathrm{SU}(2)_R \otimes \mathrm{U}(1)_B)/\mathrm{SU}(2)_{L=R} = \mathrm{SU}(2) \otimes \mathrm{U}(1)_B, \tag{5.17}$$

which transforms under global transformations of $\mathrm{SU}(2)_L \otimes \mathrm{SU}(2)_R$ as

$$U(x) \to U'(x) = RU(x)L^\dagger, \;\; R \in \mathrm{SU}(2)_R, \;\; L \in \mathrm{SU}(2)_L. \tag{5.18}$$

This field is expressed in terms of dynamic variables suitable for low-energy. For two quark flavors this means that one replaces the quark and gluon fields by pion fields: $\vec{\pi} = \{\pi_1(x), \pi_2(x), \pi_3(x)\}$. Thus, $U(x)$ is written as

$$U(x) = \exp\left(i\frac{\vec{\pi}\cdot\vec{\tau}}{F_\pi}\right), \;\; \vec{\tau} = (\sigma_1, \sigma_2, \sigma_3), \tag{5.19}$$

where F_π is known as the pion decay constant and makes the argument of the exponential dimensionless (the pion fields have dimension of mass in units of $c = \hbar = 1$) and where σ are the Pauli matrices, which are the generators of SU(2). Hence

$$U(x) = \exp\left(i\frac{\phi(x)}{F_\pi}\right), \;\; \phi(x) = \begin{pmatrix} \pi^0 & \sqrt{2}\pi^+ \\ \sqrt{2}\pi^- & -\pi^0 \end{pmatrix},$$
$$\pi^0 = \pi_3, \;\; \pi^\pm = \frac{\pi_1 \mp i\pi_2}{\sqrt{2}}. \tag{5.20}$$

$\mathcal{L}_{\text{eff}}$ is constructed by using $U(x)$. It must have all the terms that present the symmetries of QCD (e.g. Lorentz invariance, chiral symmetry, etc.). Each term is accompanied by a coefficient denominated low energy constant (LEC), that has to be determined from the

underlying theory. However, there are actually an infinite number of terms consistent with the symmetries. They can be organized in increasing powers of momentum, which is the same as increasing number of derivatives, so one can truncate them for low energy. In the massless case, the effective Lagrangian with the least number of derivatives reads

$$\mathcal{L}_{\text{eff}} = \frac{F_\pi^2}{4}\text{tr}\left(\partial_\mu U \partial^\mu U^\dagger\right). \tag{5.21}$$

The denominator 4 is because if one expands in powers of ϕ up to second order, the kinetic term $\frac{1}{2}\text{tr}(\partial_\mu\phi\partial^\mu\phi^\dagger)$ is obtained. Under the transformation of eq. (5.18) the Lagrangian is invariant

$$\mathcal{L}_{\text{eff}} = \frac{F_\pi^2}{4}\text{tr}\left(\Omega_R\partial_\mu U\Omega_L^{-1}\Omega_L\partial^\mu U^\dagger\Omega_R^{-1}\right) = \frac{F_\pi^2}{4}\text{tr}\left(\Omega_R^{-1}\Omega_R\partial_\mu U\partial^\mu U^\dagger\right) = \frac{F_\pi^2}{4}\text{tr}\left(\partial_\mu U\partial^\mu U^\dagger\right), \tag{5.22}$$

where we have used the property $\text{tr}(AB) = \text{tr}(BA)$.

If one introduces the masses m_u and m_d to the theory, a term that explicitly breaks the chiral symmetry is added

$$\mathcal{L}_{\text{s.b.}} = \frac{F_0^2 B_0}{2}\text{tr}\left(MU^\dagger - UM\right), \quad M = \begin{pmatrix} m_u & 0 \\ 0 & m_d \end{pmatrix}, \tag{5.23}$$

where s.b. stands for symmetry breaking and F_0 and B_0 are two LECs. Then, to leading order the massive effective Lagrangian reads

$$\mathcal{L}_{\text{eff}} = \frac{F_\pi^2}{4}\text{tr}\left(\partial_\mu U\partial^\mu U^\dagger\right) + \frac{F_0^2 B_0}{2}\text{tr}\left(MU^\dagger - UM\right). \tag{5.24}$$

For degenerate quark masses $m_u = m_d \equiv m$, the LECs satisfy the following relations [5]

$$\begin{aligned} F_\pi &= F_0\left[1 + O\left(\frac{m}{\Lambda_{\text{QCD}}}\right)\right], \\ \langle 0|\,\overline{q}q\,|0\rangle &= -2F_0^2 B_0\left[1 + O\left(\frac{m}{\Lambda_{\text{QCD}}}\right)\right], \\ m_\pi &= \sqrt{2B_0 m}\left[1 + O\left(\frac{m}{\Lambda_{\text{QCD}}}\right)\right]. \end{aligned} \tag{5.25}$$

In the chiral limit $F_\pi = F_0$. For $m \ll \Lambda_{\text{QCD}}$ eqs. (5.25) allow us to write $\mathcal{L}_{\text{eff}}$ in a more convenient way

$$\mathcal{L}_{\text{eff}} = \frac{F_\pi^2}{4}\text{tr}\left(\partial_\mu U\partial^\mu U^\dagger\right) + \frac{\Sigma}{4}\text{tr}\left(MU^\dagger - UM\right), \quad \Sigma \equiv -\langle 0|\,\overline{q}q\,|0\rangle \tag{5.26}$$

The effective Lagrangian can be formulated in terms of a normalized field $\vec{S}(x) \in \text{O}(4)$, $|\vec{S}(x)| = 1$ as well, since there is a local isomorphism between O(4) and $\text{SU}(2)_L \otimes \text{SU}(2)_R$. The symmetry breaking pattern takes the form

$$\text{O}(4) \to \text{O}(3) \leftrightarrow \text{SU}(2)_L \otimes \text{SU}(2)_R \to \text{SU}(2). \tag{5.27}$$

In terms of the field $\vec{S}(x)$, $\mathcal{L}_{\text{eff}}$ with the least number of derivatives reads

$$\mathcal{L}_{\text{eff}} = \frac{F_\pi^2}{2}\partial^\mu\vec{S}\cdot\partial_\mu\vec{S}. \tag{5.28}$$

Now, we introduce an external field $\vec{H}$ that explicitly breaks the symmetry by adding the term

$$\mathcal{L}_{\text{s.b.}} = -\Sigma\vec{H}\cdot\vec{S}, \tag{5.29}$$

where $\vec{H}$ plays the same role as the quark mass. This is known as the non-linear σ model [6].

5.3 Regimes of Chiral Perturbation Theory

From eq. (5.24) we see that the leading order LECs are F_π, B_0 and F_0. These constants can be determined trough lattice simulations by measuring the chiral condensate and fitting the functions in eqs. (5.25), using the known masses of the pion and the quarks. Nevertheless, one cannot simulate an infinite volume, so three regimes with finite volume in Euclidean space $V = L^{d1}$, with d the dimension, have been established. For each one of them, the relation between the LECs can be different from the one that is shown in eqs. (5.25). Still, the LECs are the same in all the regimes. Let us briefly review them:

- First we discuss the *p-regime*. It consists of a large volume compared to the correlation length: $L \gg \xi = m_\pi^{-1}$. In this regime the finite volume corrections are suppressed by a factor proportional to $\exp(-m_\pi L)$, so eqs. (5.25) are valid [5].
- If $L \lesssim \xi$ then we refer to the so-called *ϵ-regime* [7]. Here the finite volume corrections cannot be neglected. In the ϵ-regime the chiral condensate has the following dependence on the LECs, m and the volume when $B_0 m L^2 \ll 1$ (see ref. [8])

$$\langle 0|\,\overline{q}q\,|0\rangle = -2F_0^2 B_0 \left(\frac{I_1'(F_0^2 B_0 m V)}{I_1(F_0^2 B_0 m V)} - \frac{1}{F_0^2 B_0 m V}\right), \tag{5.30}$$

  where I_1 is the modified Bessel function of first kind of order one. Let us revise the infinite volume limit of this expression. For that purpose, we denote $x = F_0^2 B_0 m V$ and we use the asymptotic form of the modified Bessel functions (see e.g. ref. [9])

$$I_\nu(x) \sim \frac{e^x}{\sqrt{2\pi x}}\left(1 - \frac{4\nu^2 - 1}{8x}\right). \tag{5.31}$$

  Then

$$\frac{I_1'(x)}{I_1(x)} - \frac{1}{x} \sim -\frac{15 - 30x + 16x^2}{6x - 16x^2} = -\frac{\frac{15}{x^2} - \frac{30}{x} + 16}{\frac{6}{x} - 16}. \tag{5.32}$$

  When $x \to \infty$ the last expression converges to 1. Thus, the infinite volume limit of eq. (5.30) recovers $\langle 0|\,\overline{q}q\,|0\rangle = -2F_0^2 B_0$. On the other hand, we can find the limit of $\langle 0|\,\overline{q}q\,|0\rangle$ when $m \to 0$ at finite volume. To do that we use the following expressions for the modified Bessel functions and their derivatives

$$I_\nu(x) = \sum_{k=0}^{\infty} \frac{(x/2)^{\nu+2k}}{k!\Gamma(\nu + k + 1)}, \quad I_\nu'(x) = I_{\nu-1}(x) - \frac{\nu}{x} I_\nu(x). \tag{5.33}$$

  Then we have

$$\begin{aligned} \frac{I_1'}{I_1} - \frac{1}{x} &= \frac{I_0(x) - \frac{1}{x} I_1(x)}{I_1(x)} - \frac{1}{x} = \frac{\sum_{k=0}^{\infty} \frac{(x/2)^{2k}}{k!\Gamma(k+1)}}{\sum_{k=0}^{\infty} \frac{(x/2)^{1+2k}}{k!\Gamma(k+2)}} - \frac{2}{x} \\ &\underbrace{\approx}_{x\to 0} \frac{\frac{1}{\Gamma(1)}}{\frac{(x/2)}{\Gamma(2)}} - \frac{2}{x} = 0. \end{aligned} \tag{5.34}$$

  Hence, we see that in the chiral limit $\langle 0|\,\overline{q}q\,|0\rangle$ vanishes. This is consistent with the fact that in finite volume there is no spontaneous symmetry breaking.
- Finally, the *δ-regime* is determined by a volume of size $V = L^3 \times L_t$, where the spatial volume is small, but the Euclidean time extension is large, that is $L \lesssim \xi \ll L_t$ [10].

[1] We will take the Euclidean time extension to be equal to the spatial volume for two of the three regimes.

The pion decay constant has been calculated in the p-regime and the ϵ-regime with three flavors several times, giving a result of $F_\pi = 92.1(9)$ MeV [11, 12, 13, 14]. On the other hand, the δ-regime is less explored; there F_π has been measured with two flavors obtaining $F_\pi = 78^{+14}_{-10}$ MeV [15].

The ϵ and δ-regime are useful from a technical point of view, because the small volume reduces the computing time of the simulations. In particular, in the δ-regime the fact that $L \lesssim \xi \ll L_t$ has several effects. First, in the chiral limit the pion mass does not become massless and instead there is a *residual mass* $m_\pi^R \neq 0$. Another consequence is that there is approximately only one dimension, that enables us to treat the system as a quasi one dimensional field theory, *i.e.* quantum mechanics [10]. Then, in the O(4) model, $\vec{S}(x)$ describes approximately a particle moving in a unit sphere $\mathbb{S}^2$. One can express m_π^R as the energy gap of a quantum rotor, which is given by

$$E_j = \frac{j(j+N-2)}{2\Theta}, \tag{5.35}$$

where Θ is the moment of intertia and N refers to the group O(N). The value of Θ was computed in ref. [16] up to next-to-leading order, for a general dimension $d > 2$ and $N \geq 2$

$$\Theta = F_\pi^2 L^{d-1}\left[1 + \frac{N-2}{4\pi F_\pi^2 L^{d-2}}\left(2\frac{d-1}{d-2} + \cdots\right)\right], \tag{5.36}$$

however, the leading term had been calculated in ref. [10] for four dimensions already.

m_π^R is obtained by substituting $j = 1$ and $N = 4$ in eq. (5.35)

$$m_\pi^R = \frac{3}{2\Theta}. \tag{5.37}$$

In four dimensions we have

$$m_\pi^R = \frac{3}{2F_\pi^2 L^3(1+\Delta)}, \;\; \Delta = \frac{0.477\cdots}{(F_\pi L)^2} + \ldots, \;\; d = 4. \tag{5.38}$$

Calculations of Δ up to $1/(F_\pi L)^4$ have been done in ref. [17]. In two dimensions there is a divergence of the next-to-leading term, so instead we just consider the leading term, yielding

$$m_\pi^R \simeq \frac{3}{2F_\pi^2 L}, \;\; d = 2. \tag{5.39}$$

This dimension has not been considered in this context, because there are no NGBs [18]. Still, at finite fermion mass the lightest particles are similar to quasi NGBs and we will refer to them as pions [19]. Note that when $d = 2$ F_π is dimensionless, since the mass has units of inverse of length.

Several simulations of the two flavor Schwinger model were performed in the δ-regime with the HMC algorithm. This allowed us to obtain m_π^R as a function of L, in order to verify the relation $m_\pi^R \propto 1/L$ and extract the value of F_π from eq. (5.39) .

5.4 δ-regime results

As in Chapter 3, we will denote $\beta = 1/g^2$. All the plots shown are in lattice units, *i.e.* the lattice constant a is set to 1. To make the lattice finer, we increment the value of β. Results for $\beta = 2, 3$ and 4 were obtained through 1,000 measurements, separated by 10 sweeps. 500 sweeps were performed to thermalize the field configurations. It is important to mention that under gauge interaction the fermion mass undergoes renormalization, so

it is necessary to measure a renormalized mass m, instead of using the input mass of the simulations. This can be achieved with the *partial conservation of axial current* (PCAC) relation [20]

$$\langle \partial_\mu A^a_\mu(x) P^a(0)\rangle = 2m\langle P^a(x)P^a(0)\rangle, \tag{5.40}$$

where A^a_μ is the *isovector axial current*, P^a is the *pseudoscalar density* and m the renormalized fermion mass

$$\begin{aligned} A^a_\mu(x) &= \frac{1}{2}\overline{q}(x)\gamma_\mu\gamma_5\sigma^a q(x), \\ P^a(x) &= \frac{1}{2}\overline{q}(x)\gamma_5\sigma^a q(x), \end{aligned} \tag{5.41}$$

where σ^a denotes the Pauli matrices. Let us note that eq. (5.40) partially restores the broken axial symmetry when $m = 0$. With the PCAC relation, m_π was measured for different values of m and lattice sizes.

In figure 5.1 (a), m_π is shown as a function of the degenerate quark mass m for $L = 6$, $L_t = 64$ and $\beta = 4$. We can see that close to the chiral limit, the value of m_π becomes very unstable, so one cannot simply measure m_π at $m = 0$. Instead one extrapolates the value to $m = 0$. However, that is easier to do with figure 5.1 (b), where m_π is plotted against $(m^2 g)^{1/3}$. A function of the form $y = \sqrt{a + bx^3}$, where $x = (m^2 g)^{1/3}$ and a and b are fit parameters, was fitted to extrapolate m^R_π. Many attempts with functions of the form $y = \sqrt{a + bx^c}$ and $y = a + bx^c$ were performed. The best results were obtained by taking $c = 3$ in the former expression. We do not have an explanation for this behavior, but it works best to infer m^R_π. We make the observation that in figure 5.1 (a) there are results for negative fermion mass. In the simulation both signs are measured; nevertheless, the negative values do not have physical meaning and they were ignored in the extrapolations.

This same procedure was done for different L between 5 and 12 and $L_t = 64$. In figure 5.2 plots of m_π vs. $(m^2 g)^{1/3}$ are shown for $\beta = 2$, in figure 5.3 for $\beta = 3$ and in figure 5.4 for $\beta = 4$.

Finally, we plot m^R_π as a function of L and fit a function of the form $3/(2LF^2_\pi)$ (figures 5.5, 5.6 and 5.7).

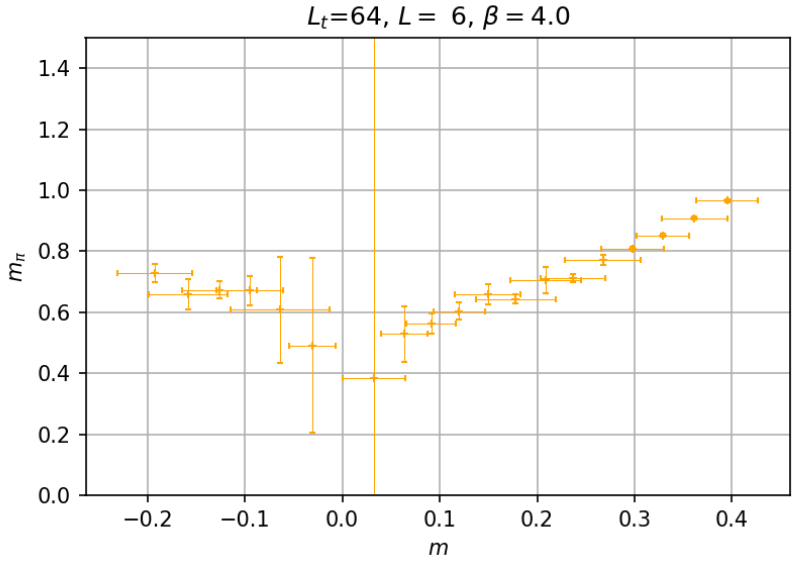

(a) m_π vs. m. We see that near $m = 0$ the pion mass result is plagued by large errors.

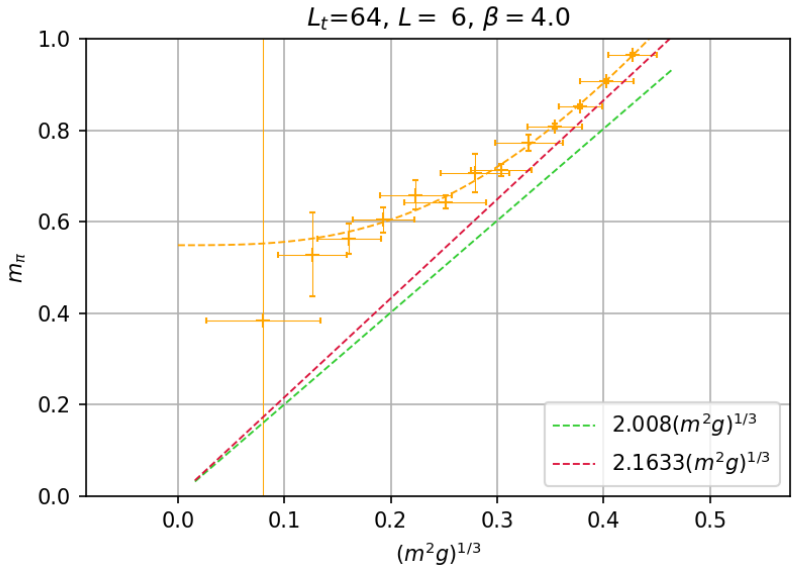

(b) m_π vs. $(m^2g)^{1/3}$. One can fit a function of the form $y = \sqrt{a + bm^2g}$ to obtain the value of the residual pion mass: $m_\pi^R = 0.549(12)$. The predictions for m_π at finite temperature, mentioned in Chapter 3, are shown as well.

Figure 5.1: Results of m_π and m. Note that there are also values for $m < 0$, they are unphysical. However, in the simulation both signs of the mass are measured. In the lower plot only $m > 0$ was considered. The errors were computed by using the *Jackknife method* (see Appendix B for the definition).

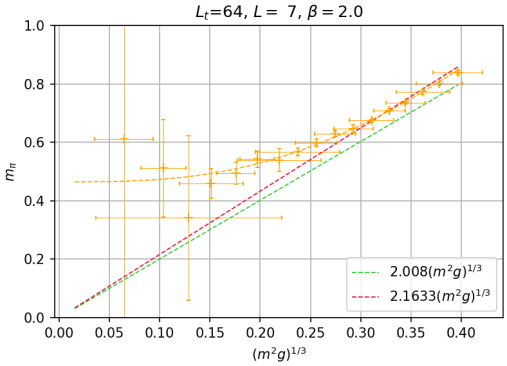

(a) m_π vs. $(m^2g)^{1/3}$ for $L = 7$. m_π =0.4645(72)

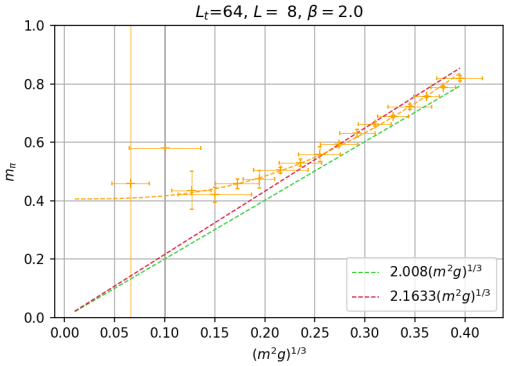

(b) m_π vs. $(m^2g)^{1/3}$ for $L = 8$. m_π =0.4063(45)

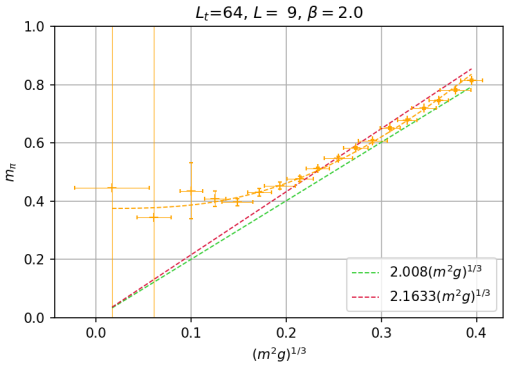

(c) m_π vs. $(m^2g)^{1/3}$ for $L = 9$. m_π =0.3749(47)

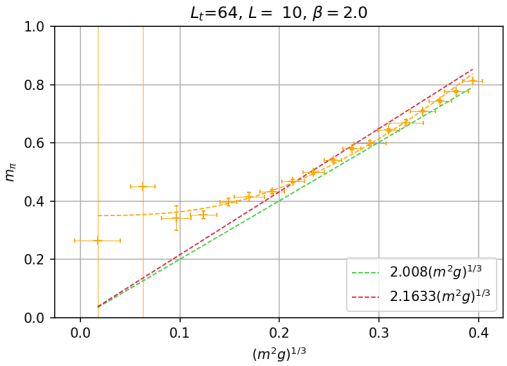

(d) m_π vs. $(m^2g)^{1/3}$ for $L = 10$. m_π =0.3505(58)

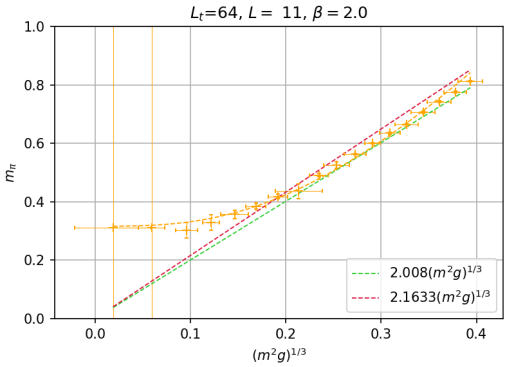

(e) m_π vs. $(m^2g)^{1/3}$ for $L = 11$. m_π =0.3163(59)

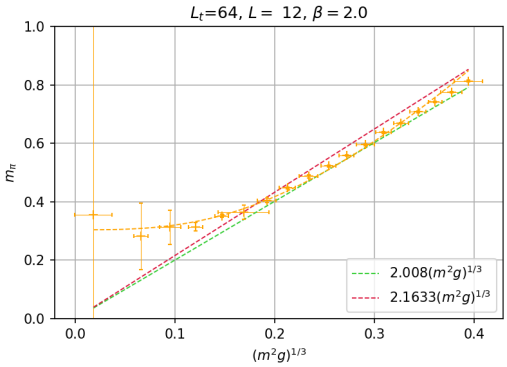

(f) m_π vs. $(m^2g)^{1/3}$ for $L = 12$. m_π =0.3040(51)

Figure 5.2: Results for $\beta = 2$. Each value of m_π and m was obtained by averaging 1,000 measurements of different configurations. Between each configuration used, 10 sweeps were performed. All the fits were made with gnuplot.

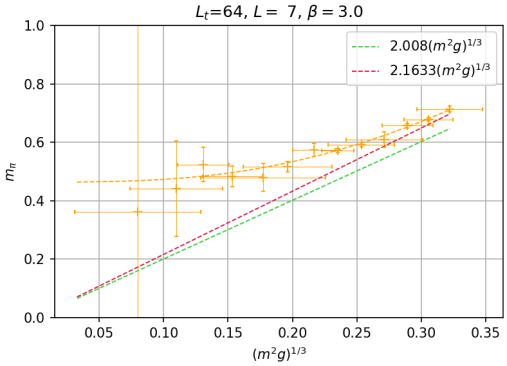

(a) m_π vs. $(m^2g)^{1/3}$ for $L = 7$. m_π =0.4639(103)

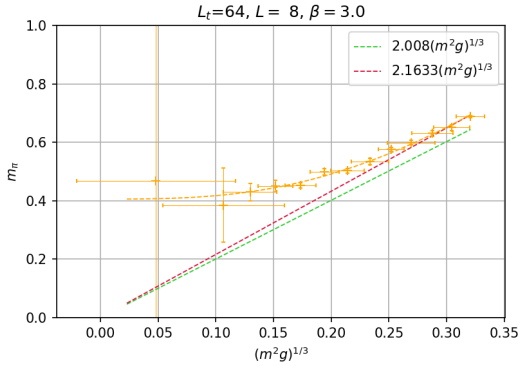

(b) m_π vs. $(m^2g)^{1/3}$ for $L = 8$. m_π =0.4057(58)

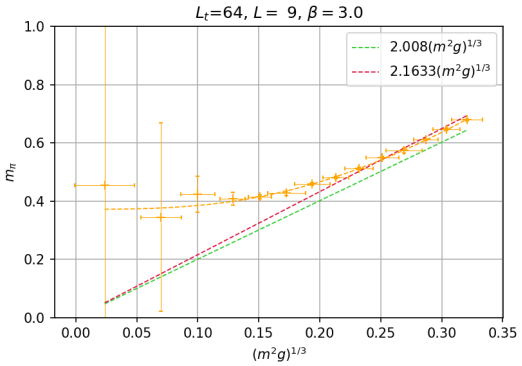

(c) m_π vs. $(m^2g)^{1/3}$ for $L = 9$. m_π =0.3722(29)

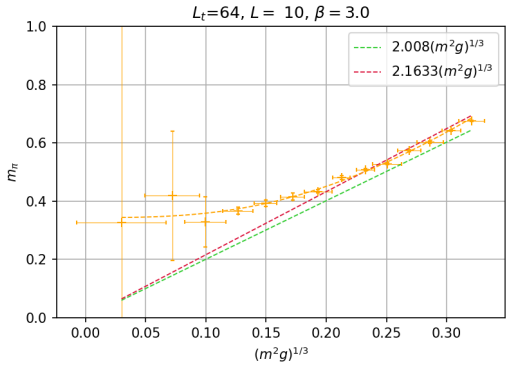

(d) m_π vs. $(m^2g)^{1/3}$ for $L = 10$. m_π =0.3437(42)

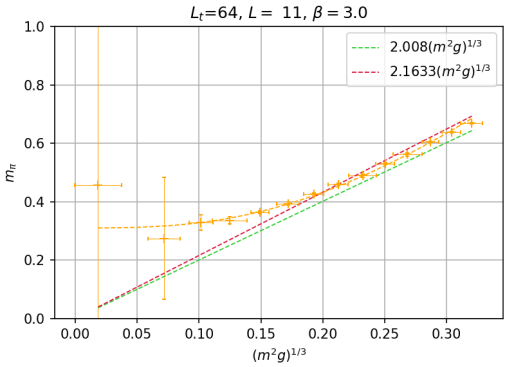

(e) m_π vs. $(m^2g)^{1/3}$ for $L = 11$. m_π =0.3104(30)

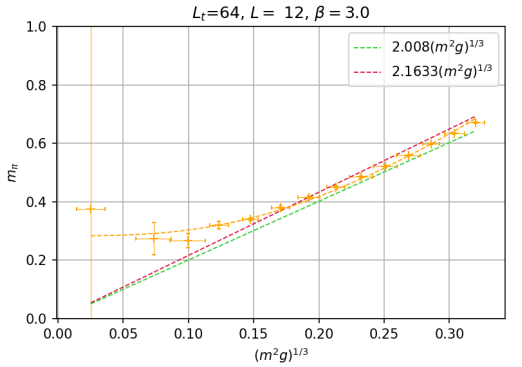

(f) m_π vs. $(m^2g)^{1/3}$ for $L = 12$. m_π =0.2832(51)

Figure 5.3: Results for $\beta = 3$. Each value of m_π and m was obtained by averaging 1,000 measurements of different configurations. Between each configuration used, 10 sweeps were performed.

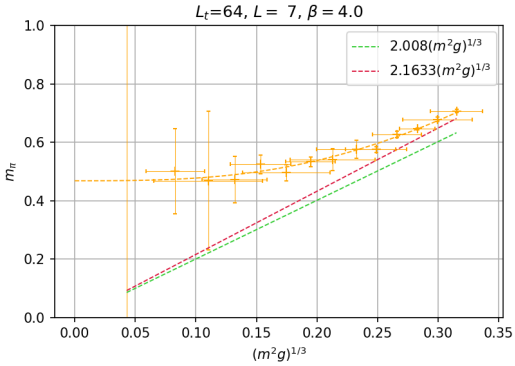

(a) m_π vs. $(m^2g)^{1/3}$ for $L = 7$. m_π =0.4684(75)

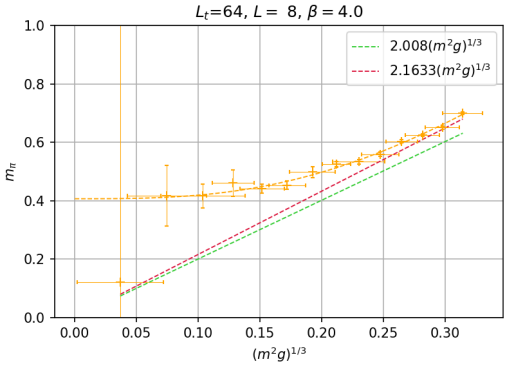

(b) m_π vs. $(m^2g)^{1/3}$ for $L = 8$. m_π =0.4068(63)

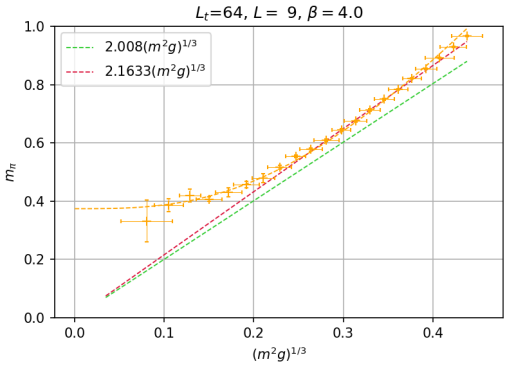

(c) m_π vs. $(m^2g)^{1/3}$ for $L = 9$. m_π =0.3741(40)

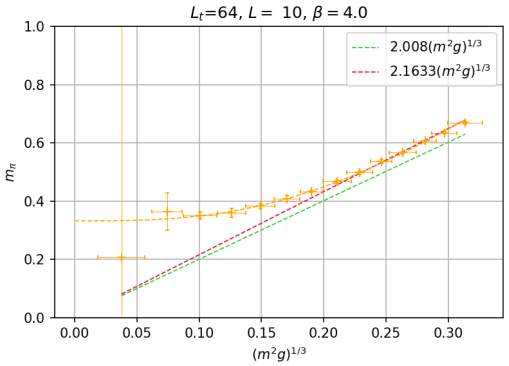

(d) m_π vs. $(m^2g)^{1/3}$ for $L = 10$. m_π =0.3323(22)

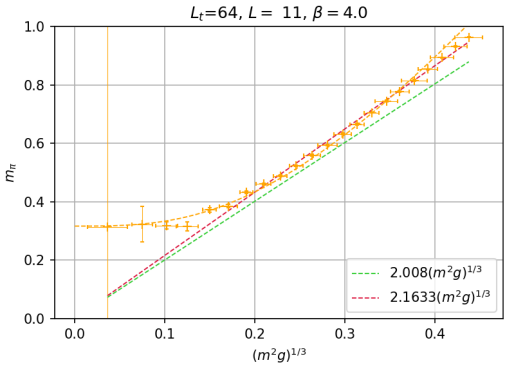

(e) m_π vs. $(m^2g)^{1/3}$ for $L = 11$. m_π =0.3167(54)

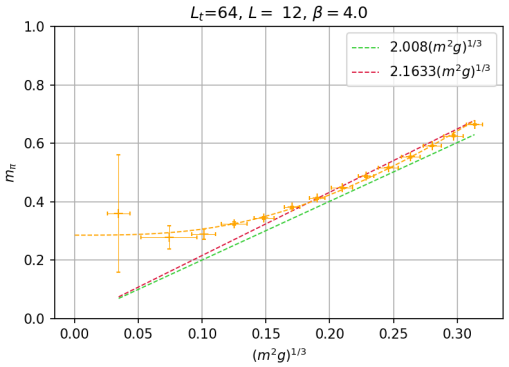

(f) m_π vs. $(m^2g)^{1/3}$ for $L = 12$. m_π =0.2857(41)

Figure 5.4: Results for $\beta = 4$. Each value of m_π and m was obtained by averaging 1,000 measurements of different configurations. Between each configuration used, 10 sweeps were performed.

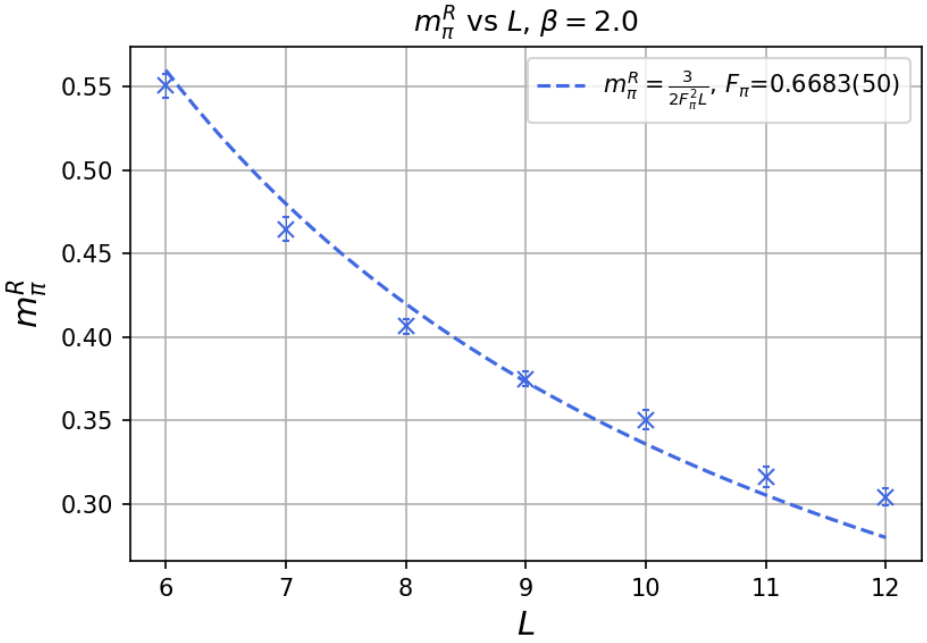

Figure 5.5: Behavior of m_π^R vs. L for $\beta = 2$.

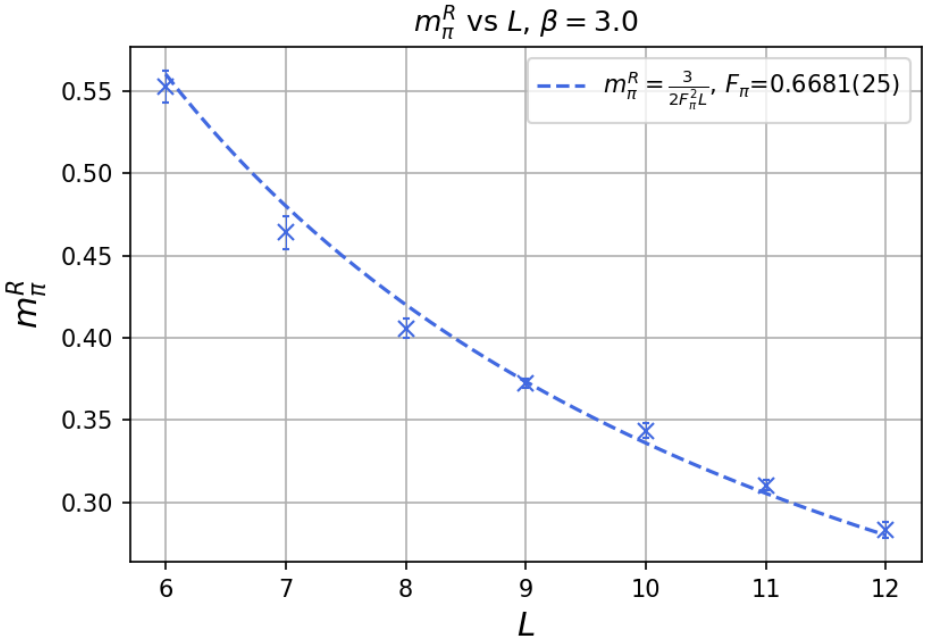

Figure 5.6: Behavior of m_π^R vs. L for $\beta = 4$. m_π^R vs. L for $\beta = 3$.

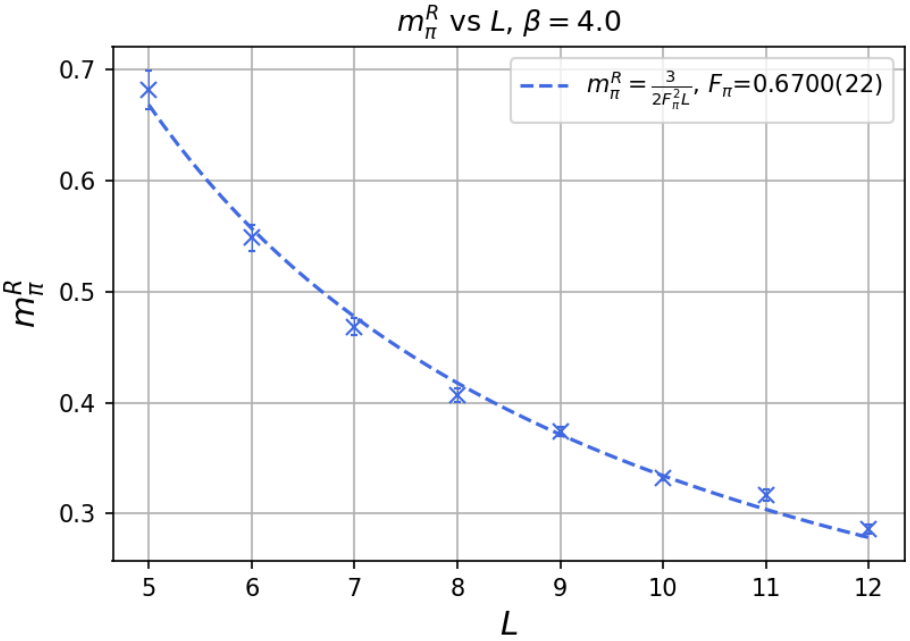

Figure 5.7: Behavior of m_π^R vs. L for $\beta = 4$. We can see that it matches the relation of $1/L$ described in eq. (5.39).

From figures 5.5, 5.6 and 5.7 we see that indeed $m_\pi^R \propto 1/L$, as the theory predicts for the δ-regime. This can be best seen for $\beta = 4$, because the lattice is finer than for $\beta = 2, 3$ and as a consequence there are less lattice artifacts. Still, for $\beta = 2, 3$ the $1/L$ relation can be seen. For all the β's used, we see that when L becomes large, m_π^R vanishes, as it should do for an infinite volume. From the fits we were able to extract F_π (see table 5.1).

β	2	3	4
F_π	0.6683(50)	0.6681(25)	0.6700(22)

Table 5.1: Pion decay constant for different values of β.

For $\beta = 4$ the error is smaller. Again, this is due to the fact that there are less lattice artifacts. An average of the values obtained for F_π yields

$$F_\pi = 0.6688(5). \tag{5.42}$$

We compare this result with the one obtained by means of the Witten-Veneziano formula in Chapter 4: $F_\pi = 0.4149(15)$. Both results differ by a factor of 1.6. This shows an inconsistency between the two methods used to measure F_π. However, the method presented in this chapter was applied to different lattice sizes and values of β, which gives more credibility. On the other hand, the computation of F_π through the topological susceptibility and the WV formula, was only done with one lattice of size $L \times L_t = 10 \times 64$ and $\beta = 4$, but with high statistics (10,000 measurements and 100 sweeps between each of them). With more measurements, the computation time of each simulation increases to several days. For that reason, there are only results for one lattice and one value of β. We attempted to measure the topological susceptibility for the statistics used in this chapter (1,000 measurements separated by 10 sweeps). Unfortunately, even though the topological charge seems to obey a Gaussian relation and is compatible with $\langle Q \rangle \approx 0$ (see figures 5.9, 5.10 and 5.11), χ_T as a function of the fermion mass m does not have a clear behavior

(see figure 5.8 for instance). This does not allow us to perform a fit and extrapolate the quenched value of χ_T. Therefore, further investigation regarding simulations with different lattice sizes and with high statistics is needed to revise whether the value of F_π obtained through the Witten-Veneziano formula is compatible with the result in the δ-regime.

The autocorrelation time τ with respect to Q (figures 5.12, 5.13 and 5.14) was measured as well (we refer the reader to Appendix C for the definition of this quantity). In some plots (e.g. figures 5.13 (b), (c), (e), (f) and 5.14 (d), (f)) we see that close to $m = 0$, the autocorrelation time has a peak. However, in some others τ is scattered. For $\beta = 4$, τ reaches maximum values beyond 14, which points out that for finer lattices the number of sweeps between each measurement should be increased in order to suppress correlations; although that also increases significantly the computing time of the simulations. For $\beta = 2$, the autocorrelation time does not have a peak and in most cases is below 2.5, which is a good sign of decorrelation. For $\beta = 3$, τ increases close to $m = 0$, but its maximum value remains below 4.

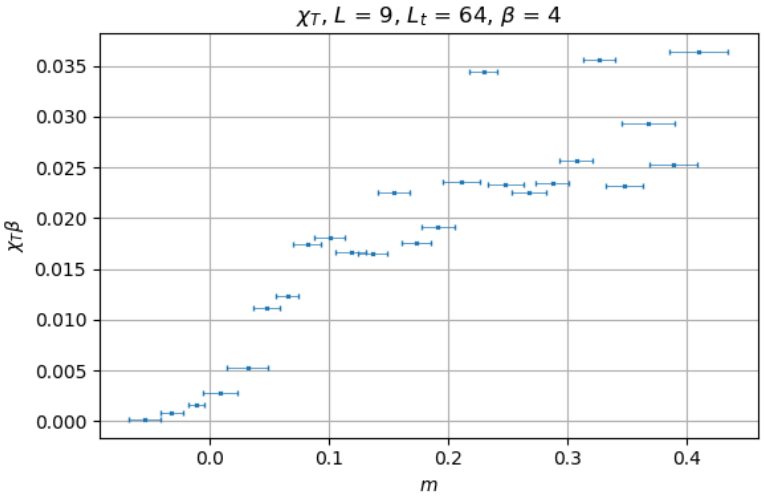

(a) χ_T for $L = 9$ and $L_t = 64$

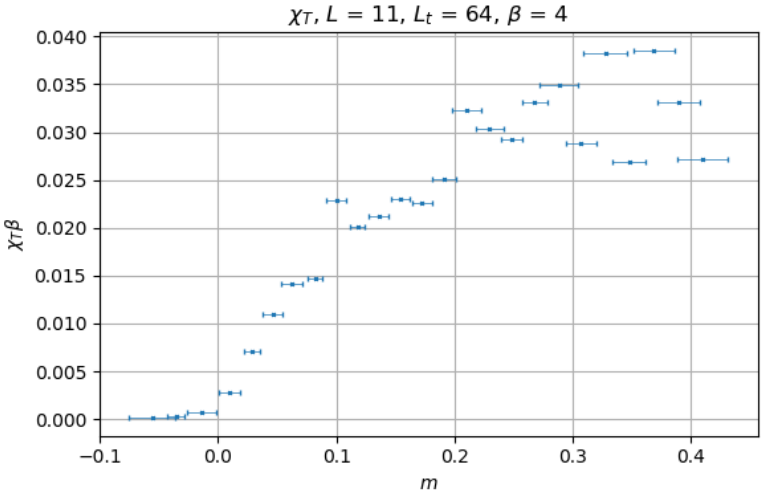

(b) χ_T for $L = 11$ and $L_t = 64$

Figure 5.8: Topological susceptibility as a function of the fermion mass m, computed for 1,000 measurements with 10 sweeps between each of them. There does not seem to be a clear behavior, in contrast with figure 4.1.

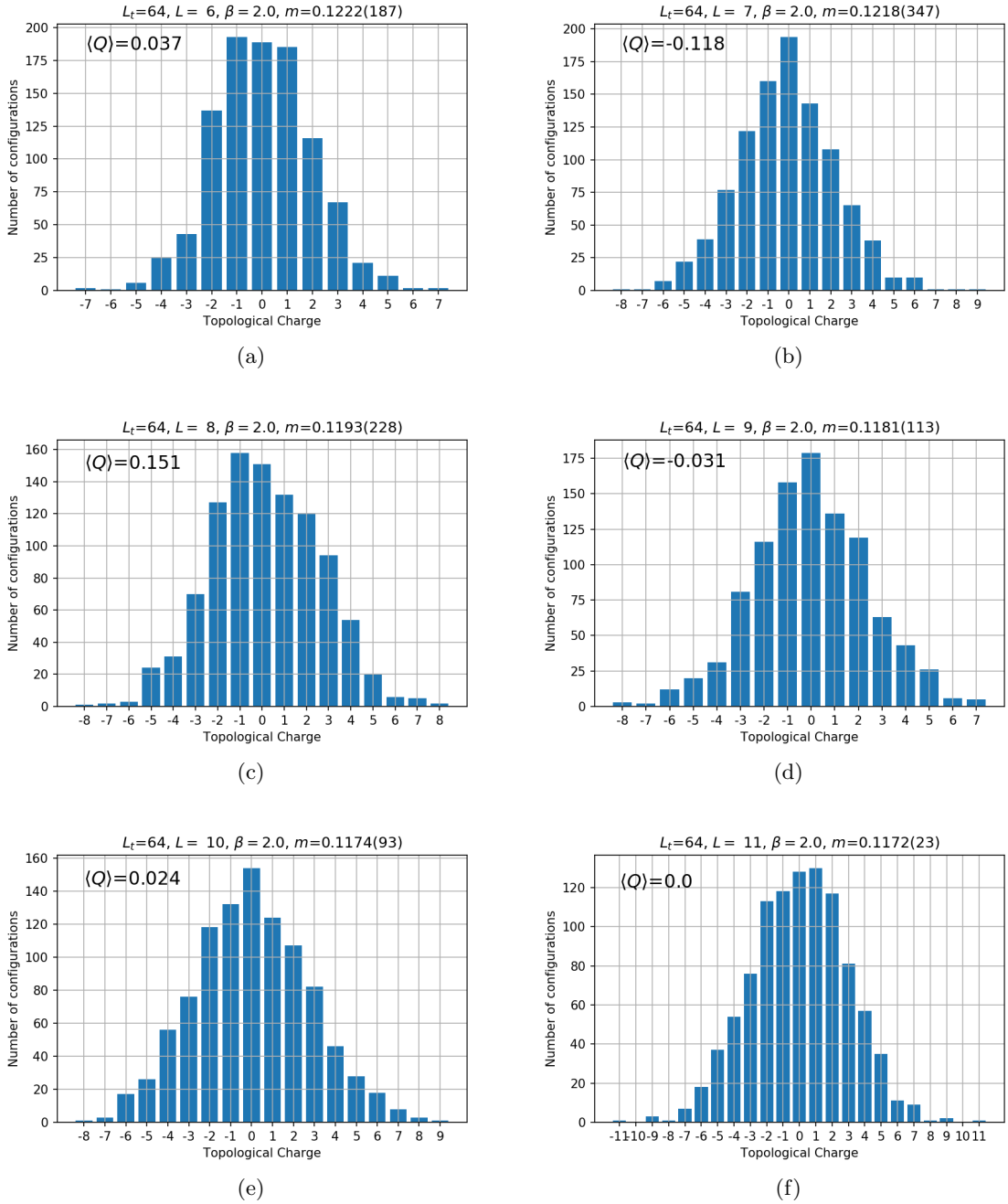

Figure 5.9: Topological charge distribution for the different lattices and fermion mass, $\beta = 2$.

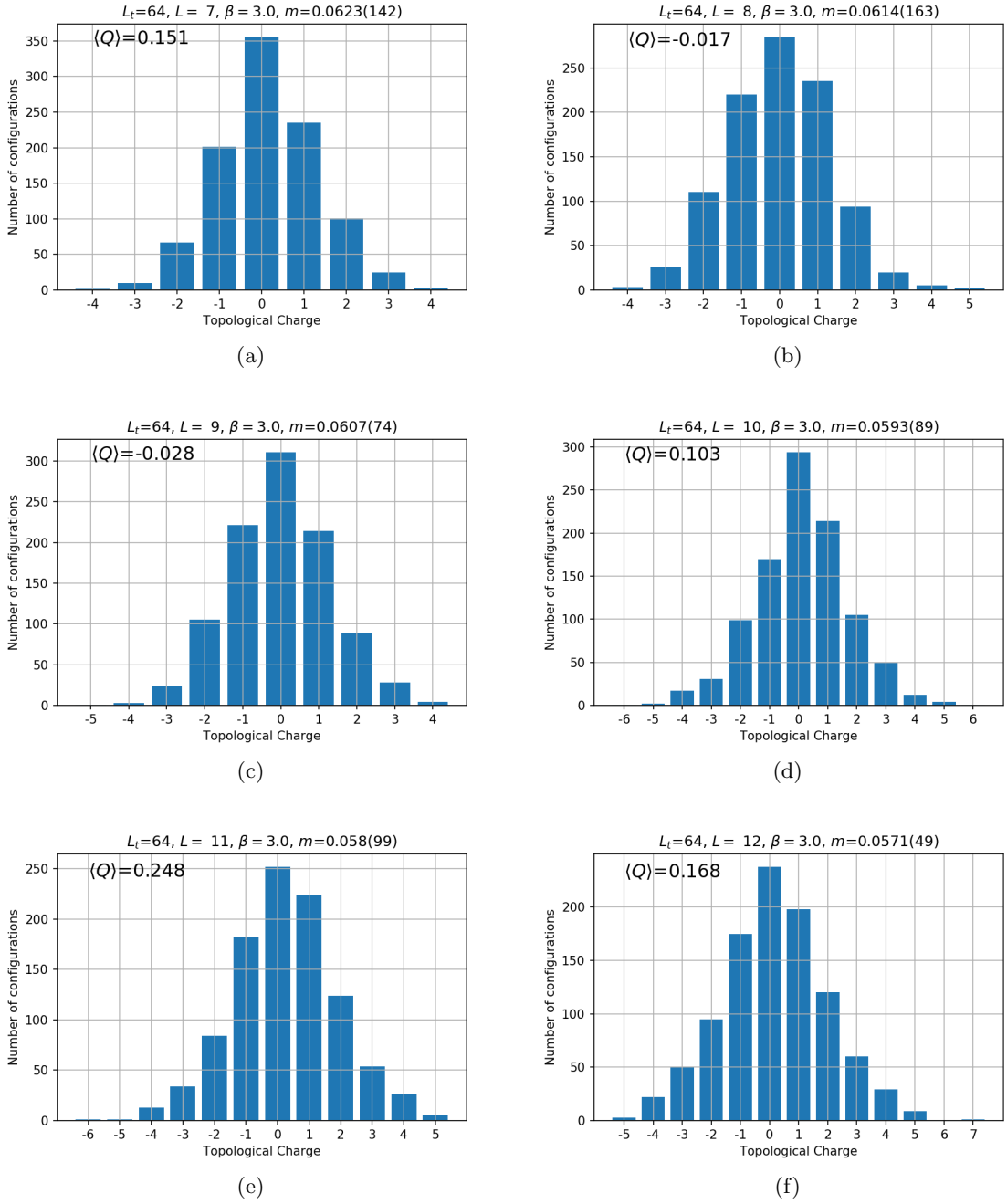

Figure 5.10: Topological charge distribution for the different lattices and fermion mass, $\beta = 3$.

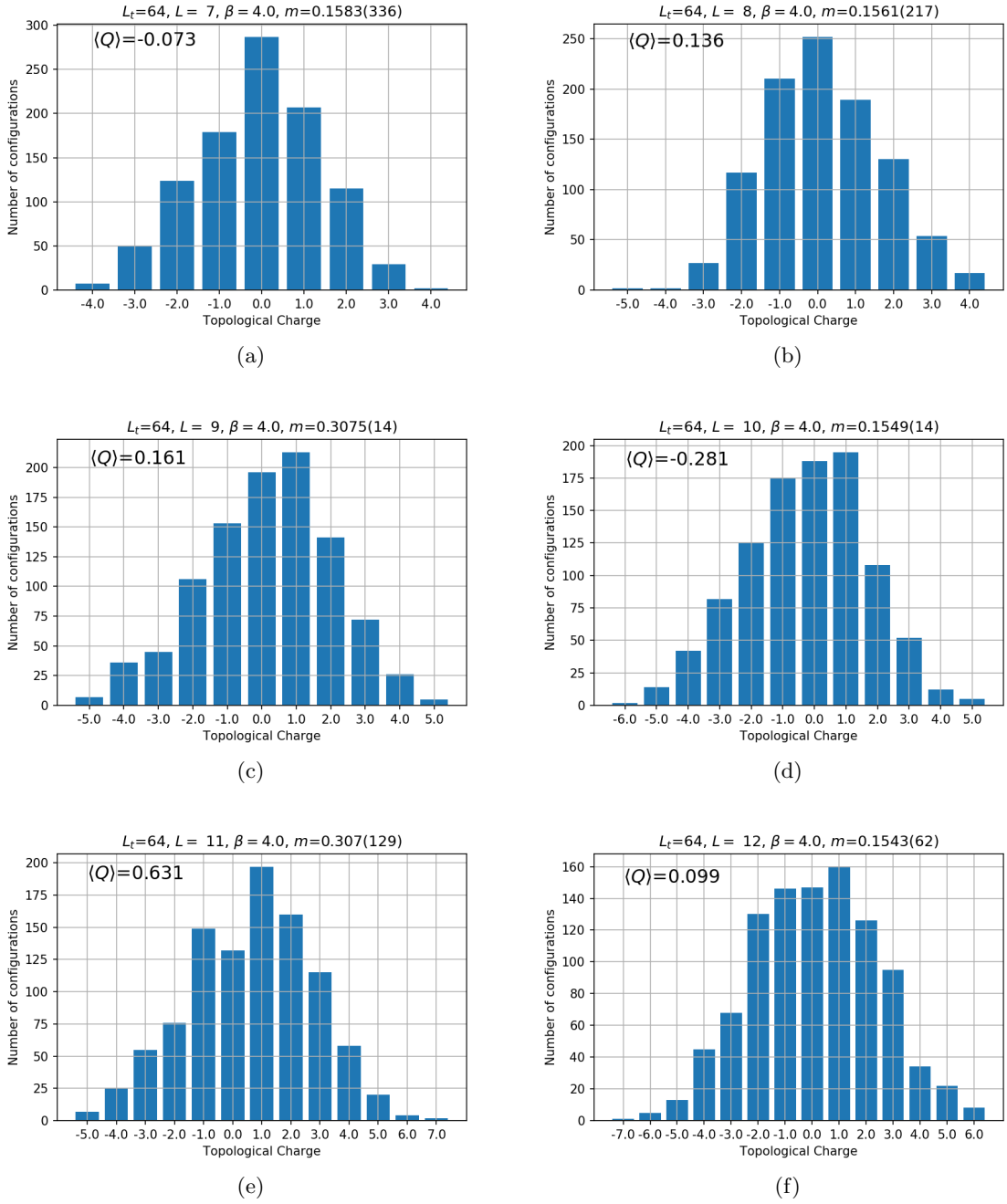

Figure 5.11: Topological charge distribution for the different lattices and fermion mass, $\beta = 4$.

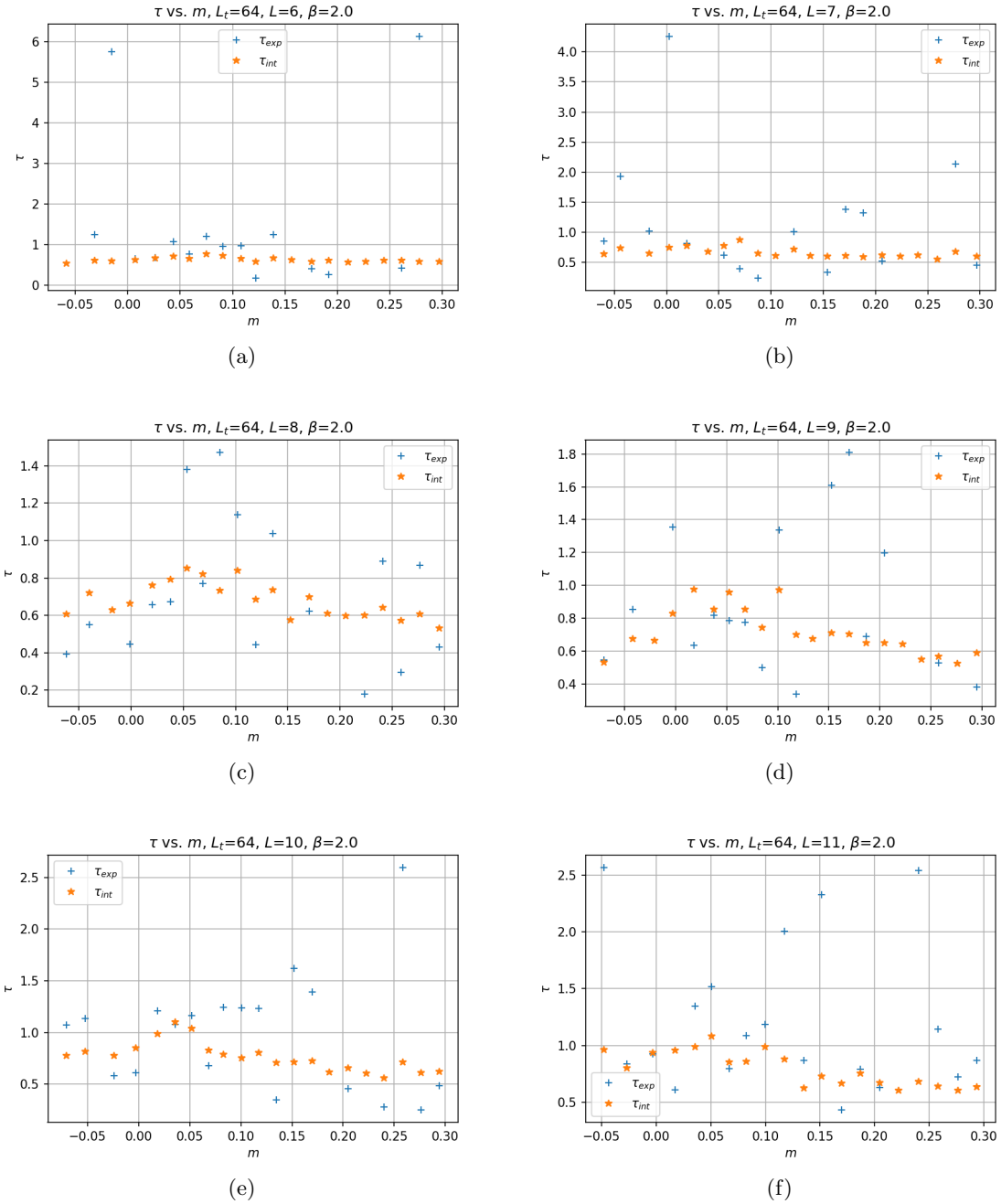

(a) (b) (c) (d) (e) (f)

Figure 5.12: Exponential and integrated autocorrelation time of the topological charge for different lattices, $\beta = 2$.

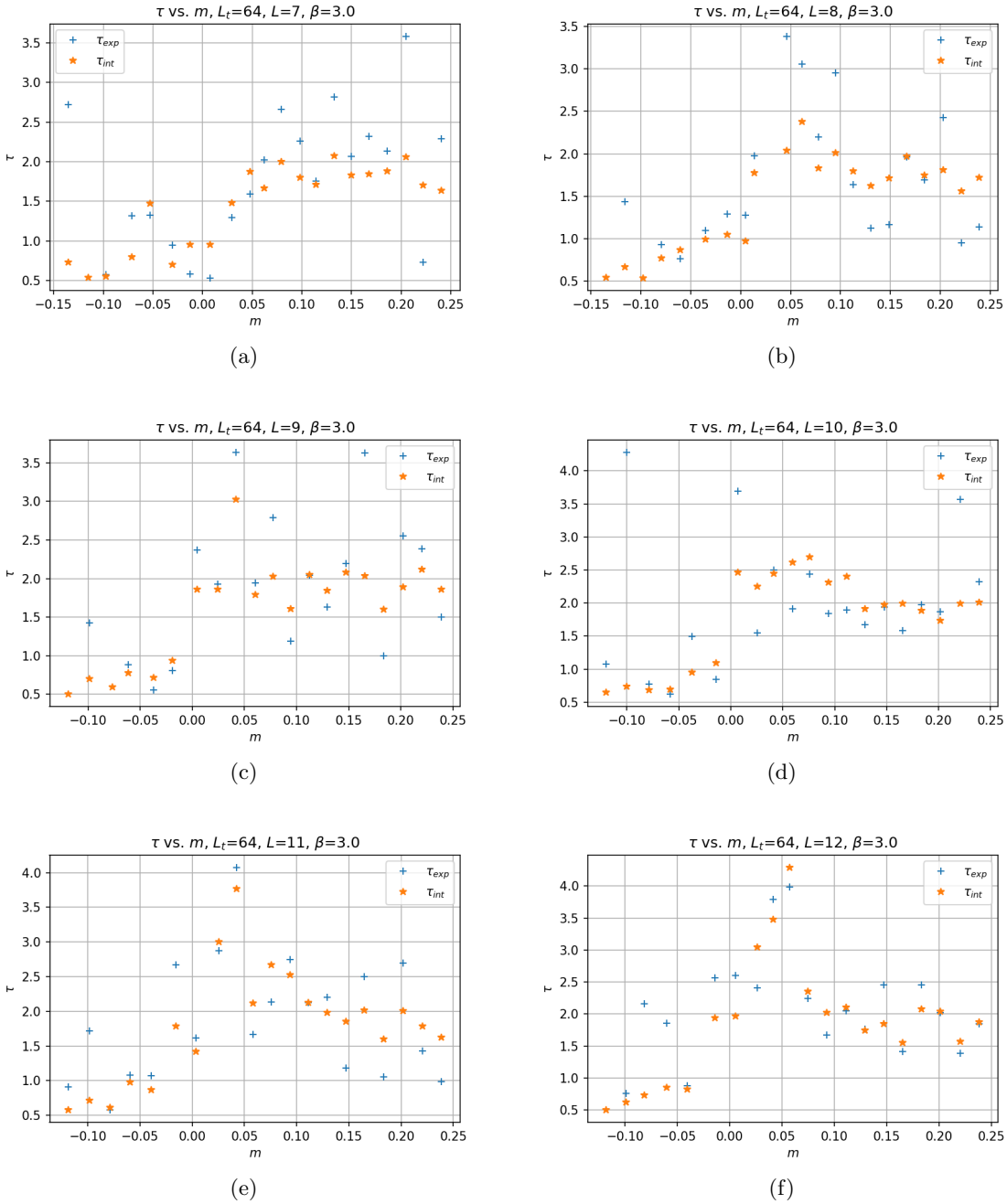

(a) (b) (c) (d) (e) (f)

Figure 5.13: Exponential and integrated autocorrelation time of the topological charge for different lattices, $\beta = 3$.

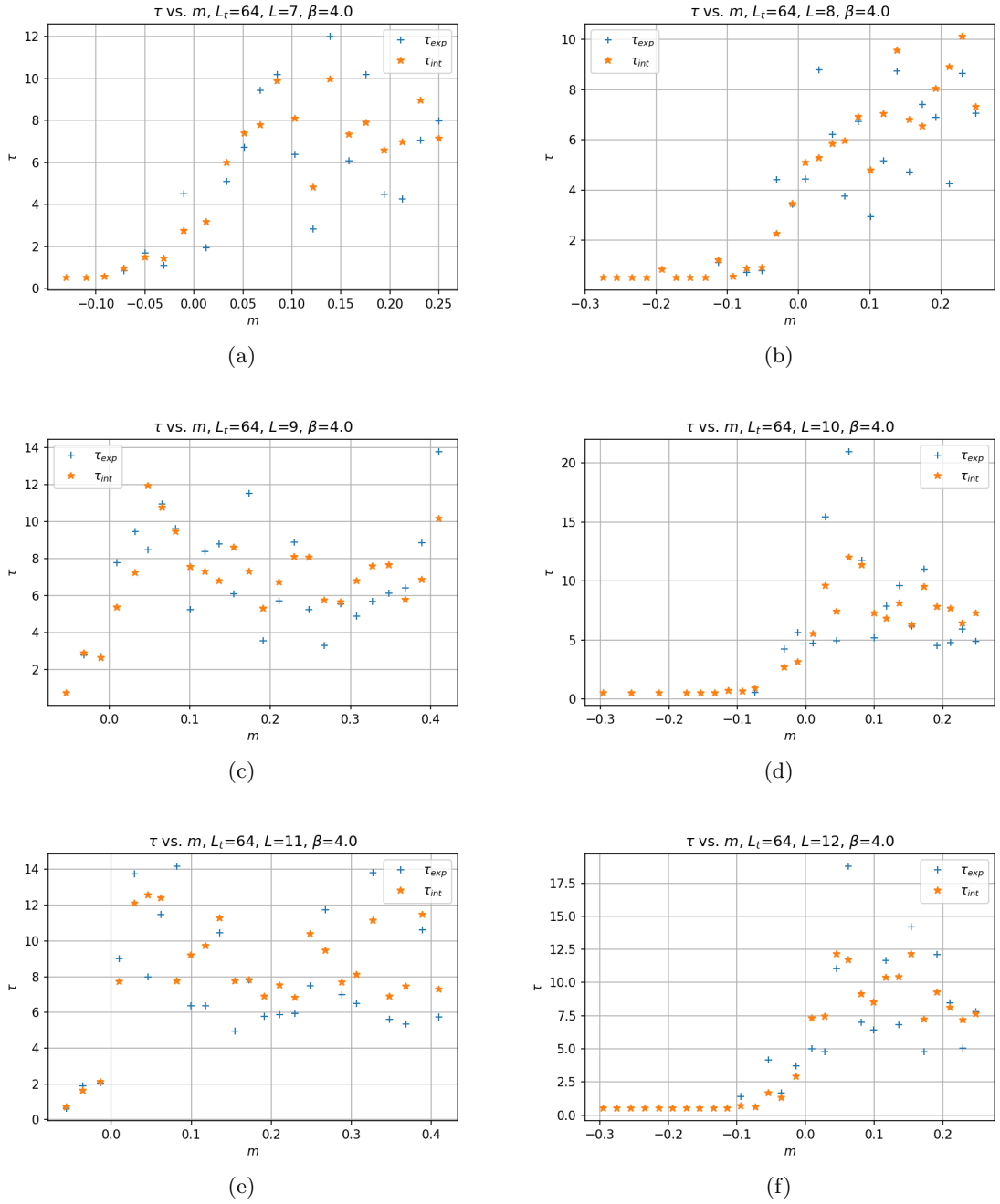

(a) (b) (c) (d) (e) (f)

Figure 5.14: Exponential and integrated autocorrelation time of the topological charge for different lattices, $\beta = 4$.

Bibliography

[1] P.A. Zyla et al. Review of Particle Physics. *Prog. Theor. Exp. Phys.*, 2020(8):083C01, 2020.

[2] S. Scherer and M. R. Schindler. *A Primer for Chiral Perturbation Theory*. Springer, 2012.

[3] A. Pich. Chiral perturbation theory. *Rept. Prog. Phys.*, 58:563–610, 1995.

[4] H. Leutwyler. Chiral perturbation theory. *Scholarpedia*, 7(10):8708, 2012.

[5] J. Gasser and H. Leutwyler. Light Quarks at Low Temperatures. *Phys. Lett. B*, 184:83–88, 1987.

[6] P. Hasenfratz and H. Leutwyler. Goldstone Boson Related Finite Size Effects in Field Theory and Critical Phenomena With O(N) Symmetry. *Nucl. Phys. B*, 343:241–284, 1990.

[7] J. Gasser and H. Leutwyler. Thermodynamics of chiral symmetry. *Phy. Lett. B*, 188(4):477–481, 1987.

[8] M. Golterman. Applications of Chiral perturbation theory to lattice QCD. In *Les Houches Summer School: Session 93: Modern perspectives in lattice QCD: Quantum field theory and high performance computing*, pages 423–515, 12 2009.

[9] M. Abramowitz and I. A. Stegun. *Handbook of Mathematical Functions with Formulas, Graphs, and Mathematical Tables*. Dover, New York, ninth dover printing, tenth gpo printing edition, 1964.

[10] H. Leutwyler. Energy Levels of Light Quarks Confined to a Box. *Phys. Lett. B*, 189:197–202, 1987.

[11] S. Aoki et al. Review of lattice results concerning low-energy particle physics. *Eur. Phys. J. C*, 77(2):112, 2017.

[12] A. Bazavov et al. Results for light pseudoscalar mesons. *PoS*, LATTICE2010:074, 2010.

[13] R. Arthur, T. Blum, P. A. Boyle, N. H. Christ, N. Garron, R. J. Hudspith, T. Izubuchi, C. Jung, C. Kelly, A. T. Lytle, R. D. Mawhinney, D. Murphy, S. Ohta, C. T. Sachrajda, A. Soni, J. Yu, and J. M. Zanotti. Domain wall QCD with near-physical pions. *Phys. Rev. D*, 87:094514, May 2013.

[14] E. Follana, C. T. H. Davies, G. P. Lepage, and J. Shigemitsu. High-Precision Determination of the π, K, D, and D_s Decay Constants from Lattice QCD. *Phys. Rev. Lett.*, 100:062002, Feb 2008.

[15] W. Bietenholz, M. Göckeler, R. Horsley, Y. Nakamura, D. Pleiter, P.E.L. Rakow, G. Schierholz, and J.M. Zanotti. Pion in a box. *Phy. Lett. B*, 687(4):410–414, 2010.

[16] P. Hasenfratz and F. Niedermayer. Finite size and temperature effects in the AF Heisenberg model. *Z. Phys. B*, 92:91, 1993.

[17] P. Hasenfratz. The QCD rotator in the chiral limit. *Nucl. Phys. B*, 828:201–214, 2010.

[18] S. R. Coleman. There are no Goldstone bosons in two-dimensions. *Commun. Math. Phys.*, 31:259–264, 1973.

[19] A. V. Smilga and J. J. M. Verbaarschot. Scalar susceptibility in QCD and the multiflavor Schwinger model. *Phys. Rev. D*, 54:1087–1093, 1996.

[20] M. Bochicchio, L. Maiani, G. Martinelli, G. C. Rossi, and M. Testa. Chiral Symmetry on the Lattice with Wilson Fermions. *Nucl. Phys. B*, 262:331, 1985.